Total yield and polar-angle distributions of biomolecules sputtered by fast heavy ions

J. Eriksson, P. Demirev, P. Håkansson, R. M. Papaléo, and B. U. R. Sundqvist
Division of Ion Physics, Department of Radiation Sciences, Uppsala University, Box 535, S-751 21 Uppsala, Sweden
(Received 4 June 1996)

Direct measurements of the number of peptide molecules ejected per fast heavy ion impact (total yield) and data on polar-angle distributions of the total amount of sputtered bioorganic material are presented. These data allow direct comparisons with sputtering models and provide information complementary to that obtained by conventional experiments on the fraction of sputtered material ejected in the form of molecular ions. Solid targets composed of the peptide tri-leucine ($m=357$ u) were irradiated by 55-MeV ^{127}I ions incident at an angle of 51° with respect to the target surface normal. The sputtered material was collected on silicon plates placed in various configurations in front of the target. The collectors were subsequently analyzed by two different methods: time-of-flight mass spectrometry and amino acid analysis. A total yield of $(3.5\pm0.7)\times10^3$ tri-leucine molecules per incident ion was measured, which corresponds to a volume of about 2×10^3 nm^3 of target material removed in a single ion impact. In the plane of ion incidence, i.e., the plane encompassing the ion incidence direction and the surface normal, the polar-angle distribution was asymmetric with respect to the surface normal and peaked away from the direction of the incoming ions. In the plane containing the surface normal and perpendicular to the plane of incidence, the ejected material displayed a symmetric and normally peaked polar-angle distribution. Comparisons of data from the two methods of collector analysis suggest that the total sputtering yield is dominated by clusters of molecules. Asymmetric angular distribution and extensive cluster ejection support hydrodynamic-type sputtering models which assume impulsive radial expansion of the solid around the incident ion path. [S0163-1829(96)09245-4]

INTRODUCTION

The method of generating gas-phase molecular ions by high stopping power (1–10 keV/nm) fast ions ($v \gg v_{\mathrm{Bohr}}$) impinging on bioorganic solids is routinely applied in biological mass spectrometry.[1,2] A fast ion deposits its energy into a narrow track mainly by collision with target electrons. The transport of energy out from the narrow track has been analyzed theoretically[3] and recently also by direct experiments.[4] However, the conversion of the electronically deposited energy into atomic motion is still an issue under consideration and a complete picture of the mechanisms underlying the fast-ion-induced ejection of intact large organic molecules is lacking. Some of the models[5,6] proposed for describing fast-ion-induced sputtering are similar to models proposed for explaining damage and latent track formation in solids.[7–9] Other models are focused more specifically on the material ejection from condensed gases or organic solids.[10–16] The models differ in predictions of, e.g., the *total yield* (the number of molecules sputtered per ion impact) dependence on the ion stopping power (dE/dx), and in predicted angular and energy distributions of sputtered material. Most models consider the ejection of neutral particles whereas most experiments are performed on ions—a discrepancy which hinders the comparison between theory and experiments.[17] For example, a key experiment such as determining the angular distribution of the ejecta has been performed only for molecular *ions* of amino acids.[18] Initial distributions of one velocity component parallel to the target surface have also been measured for a number of sputtered biomolecular ions.[19,20] In cases where comparisons between the total ejection and the ion ejection are possible clear differences are observed. The total yield obeys a steeper power-law scaling with dE/dx than the molecular ion yield for an amino-acid target.[21] Furthermore, collector experiments[22] on the fast-ion-induced sputtering of an amino-acid target reveal that the gas-phase biomolecular ions exploited in mass spectrometers represent only a small fraction (10^{-4}) of the total yield. Scanning force microscopy (SFM) images of various surfaces,[23–31] including biomolecular surfaces, bombarded by fast ions show that the material response to each ion impact is a persistent localized defect, which for an amino-acid target has a craterlike shape and a size corresponding to a high total yield (10^3–10^4).[28,30] Crater volumes measured by SFM on an amino-acid target exhibit the same dE/dx dependence as total yields determined by collector methods.[21,30] The observation that thousands of biomolecules are ejected per impact with a sensitivity to dE/dx suggests that fast ions might also be useful for modifying surfaces in a controlled way on the nanometer scale.

Below we present results of collector experiments that provide the data on the angular distribution of the *total* bioorganic material sputtered by fast heavy ions. Moreover, the total yield of a *peptide*, i.e., a biomolecule composed of a chain of amino acids, was directly measured. The polar-angle-resolved total yield data provide a possibility to compare experimental data with models and molecular-dynamics simulations.[32] Contributions to the total yield from ejected *clusters* are known to be of great importance for fast-ion-induced sputtering of inorganic targets[33–35] and the data presented in this paper allow such cluster ejection phenomena to be discussed also for organic targets.

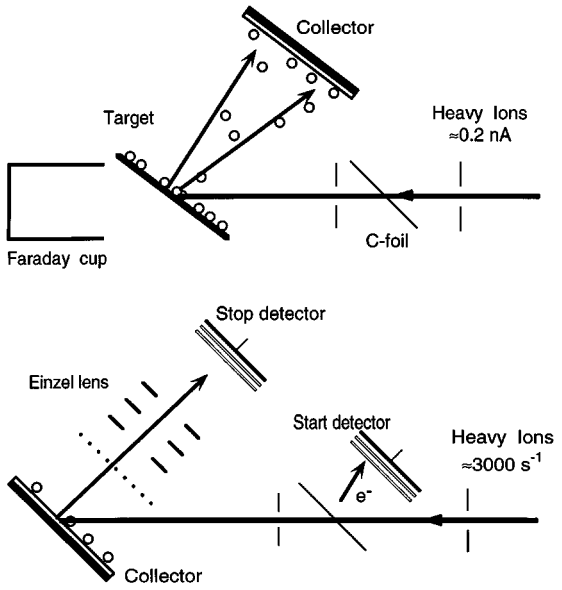

FIG. 1. The upper part is a schematic of the setup during irradiation and collection. The lower part shows the setup during collector analysis by time-of-flight mass spectrometry (PDMS).

EXPERIMENTAL

Collector methods and analysis

Collector methods are frequently employed in sputtering studies.[22,30,31,33,36] Here, peptide targets were irradiated by a 55-MeV ^{127}I ion beam while the sputtered material was collected on plates at various locations in front of the target. The area and location of each collector plate correspond to an interval of sputtering angles with respect to the target surface normal. Two independent methods of subsequent collector analysis were utilized: time-of-flight mass spectrometry (PDMS) and amino-acid analysis.

In the PDMS analysis the collectors were positioned to face the 55-MeV ^{127}I ion beam at a 45° incidence angle and the acceleration grid of the spectrometer (Fig. 1). Incident ion rates during analysis were $\approx$3000 s^{-1}. In the mass spectrum acquired from each collector surface the molecular ion peak area, subtracted for background and divided by the number of incident ions (start pulses), was determined. These data, henceforth referred to as the PDMS signal, were employed as a relative measure of the amount of bioorganic material deposited on the respective collector surface.

Amino-acid analysis (AA) is a method widely used in biochemistry in order to measure the absolute number of intact amino-acid molecules in a sample. In AA, peptides are separated into free amino acids in a solution by hydrolysis before the amount of each constituent amino acid is detected. In our case the hydrolysis also removed all biomolecules from the collector surface to the solution.[22] The collectors were analyzed with a commercial amino-acid analyzer instrument (LKB Inc., Sweden). The principle and performance of AA instrumentation are described in detail elsewhere.[37]

Targets

Targets of peptide tri-leucine (leu_3, $m=357$ u, Sigma Chemical Company, St. Louis, USA) were prepared by dissolving the molecules in acetic acid and trifluoroacetic acid (4:1) at a concentration of 10 mg/ml and then electrospraying[38,39] the solution onto silicon pieces to form a thick (>1 μm) film. The leu_3 molecule has the advantage of giving a threefold amplification of the AA signal for each intact peptide collected. The target pieces were mounted on a metal plate placed on a manipulator in the experimental chamber (turbomolecular pump, $P=1$–2×10^{-6} torr). The manipulator allowed sequential ion beam irradiation of pristine portions of the target.[30,31] The target holder could easily be removed from the beam path in order to measure the beam current in a Faraday cup placed $\approx$1 cm behind the target.

Collector surfaces

Collector plates were prepared from doped silicon pieces which were first cleaned in a basic solution of NH_4OH, H_2O_2, and H_2O (1:1:3), and afterwards in an acidic solution of HCl, H_2O_2, and H_2O (1:1:3). The solutions were held at a temperature of 80 °C during cleaning. Each cleaning step was followed by rinsing in de-ionized water. This is a standard silicon cleaning procedure[40] but leaving out the step involving hydrofluoric acid etching of the oxide layer.

Two types of metal collector holders were employed in various parts of the experiment. One type of holder consisted of two perpendicular semicircular arms (Fig. 2) approximating two $(\pi r)\times8$ mm^2 bands on a hemispherical surface of radius $r=20$ mm, where $r=0$ is the target position. The silicon pieces mounted in this holder had dimensions 4×10 mm^2 (in one experiment 3.5×10 mm^2). The two bands of collectors will henceforth be referred to as x and y. Band x represents the plane encompassing the ion incidence direction and the surface normal (xz plane), while band y represents the plane encompassing the surface normal and perpendicular to the ion incidence plane (yz plane). Using a semicircular shape we obtained the same solid angle element size and the same collector incidence angle for the ejecta at all sputtering angles. The latter is important, e.g., in case the sticking probability would depend on the angle with respect to the collector surface at which the ejecta land. A collimator ($\phi=1.5$ mm) at an angle of 51° with respect to the target surface normal on one of the collector holder arms (x) allowed passage of the primary ion beam.

In some parts of the experiment a flat holder placed at a distance of 6 mm in front of the target was employed instead. A manipulator allowed this holder to be translated perpendicularly to the beam and rotated. By translation and employing an optional slit collimator between the target and the collector, multiple collector portions could be employed independently during one experimental session without breaking vacuum. By rotation the collector surface could be positioned to face the analysis beam and the mass spectrometer (Fig. 1).

Characterization of the target

The sputtering yield from biomolecular and other targets is known to drop off during irradiation due to processes re-

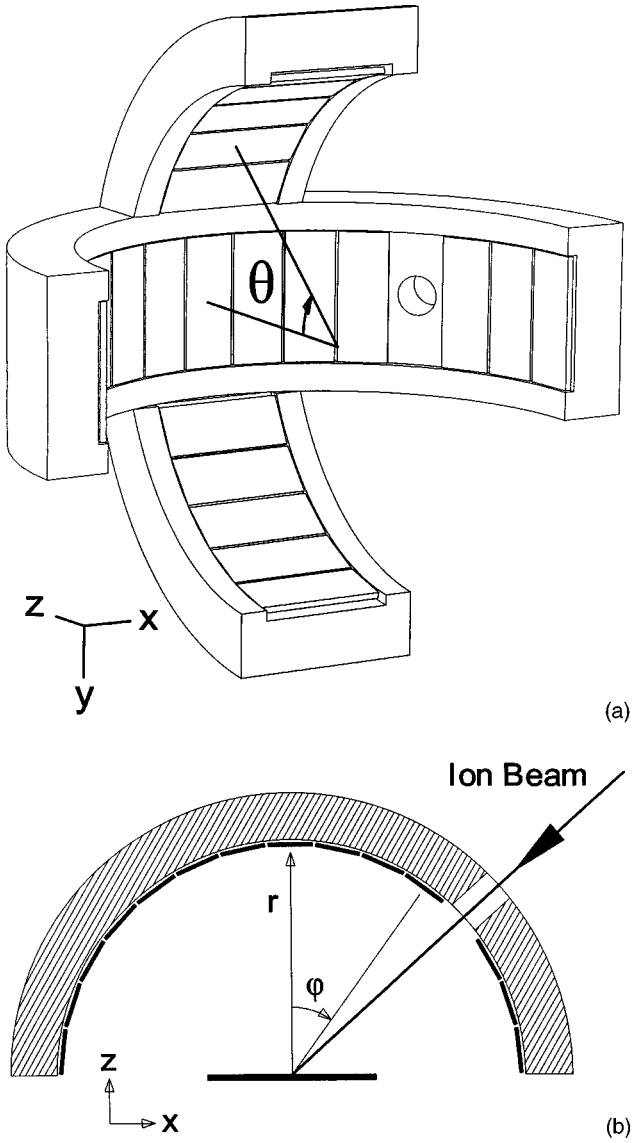

FIG. 2. Drawing of the hemispherical collector with coordinate systems and sputtering angles θ and φ marked.

ferred to collectively as radiation-induced damage.[31,41,42] The signal disappearance is characterized by a damage cross section σ. At first approximation the yield as a function of primary ion fluence ϕ [ions/cm^2] is $Y=Y_0e^{-\sigma\phi}$, where Y_0 is the yield from a pristine target spot. A collector is an integrator of the sputtering yield. Therefore a collector employed at the fluence interval $[\phi_i,\phi_{i+1}]$ probes:

$$I_i \propto \int_{\phi_i}^{\phi_{i+1}} Y_0 e^{-\sigma\cdot\phi} d\phi. \quad (1)$$

In order to determine σ and thus Y_0, a new collector was employed for each step in a sequence of irradiations of the same target spot by 55-MeV ^{127}I ions. The signal I_i from each collector was measured by PDMS.

The collector signal dependence on target irradiation current density j was also measured. For each j (15, 30, and 60 pA/mm^2), three pristine target spots were irradiated. The fluence ϕ per target spot was kept constant and a new collector was employed for each j. The PDMS signal of collectors employed at each respective j was measured. This procedure probed the influence on the measurements by macroscopic phenomena such as beam-induced temperature rise and surface charging. All target characterization experiments were performed with the flat collector holder and with PDMS analyses performed directly after the irradiations without breaking the vacuum.

Characterization of the collector response

A necessary condition for a reliable collector experiment is that one must have knowledge of the dependence of the signal from the collector on the amount of material deposited on the collector surface. For instance, for amino acid leucine ($m=131$ u) (Ref. 21) as well as peptide luteinizing hormone releasing hormone ($m=1182$ u) (Ref. 31) targets, the signal scales linearly with deposited material, except at very high collector deposition where the leucine PDMS signal saturates.[21] In order to investigate this dependence for leu_3 we irradiated several identical pristine target portions with the same ϕ, employing the *same* collector. At certain intervals of the irradiation sequence we interrupted and acquired a mass spectrum of the collector surface. In this way we probed the collector response to the deposition of leu_3 molecules on the collector surface.

A similar response measurement also considering possible response variations between collectors was performed by checking the PDMS signal from *various* collectors employed during irradiation of several identical, pristine target portions, with ϕ per target portion kept constant. In all collector response characterization experiments the flat collector holder was employed and PDMS analyses were performed directly after the irradiations with no changes of vacuum conditions.

Angular distribution and total yield measurements

Two 1.5-mm ion beam collimators, one on the hemispherical collector and another placed at a distance of 0.5 m before the target, were carefully aligned with the aid of a theodolite. The targets were irradiated by charge-equilibrated[43] 55-MeV ^{127}I ions at a current density $j\approx50$ pA/mm^2, and an incidence angle of 51° with respect to the target surface normal. Several target spots were irradiated in order to avoid excessive target damage. The beam current was measured several times during the irradiation. After the irradiations the vacuum was broken and the collectors were dismounted from the hemispherical holder and remounted onto the flat holder for subsequent analysis. Time-of-flight mass spectra from each collector piece were acquired so that a molecular ion peak, $(leu_3+H)^+$, with a satisfactory signal-to-noise ratio, was observed. In the first experiment only the x distribution was measured. The experiment was repeated and the y distribution was probed along with the x distribution. A current density $j\approx25$ pA/mm^2 was used and better angular resolution was achieved by the use of narrower collector pieces.

In order to obtain an angular distribution independent of PDMS and also to measure an absolute value of the total sputtering yield, AA of the collectors was employed in a separate experiment. Irradiation ($j\approx55$ pA/mm^2) and collection were performed as described above but the collectors

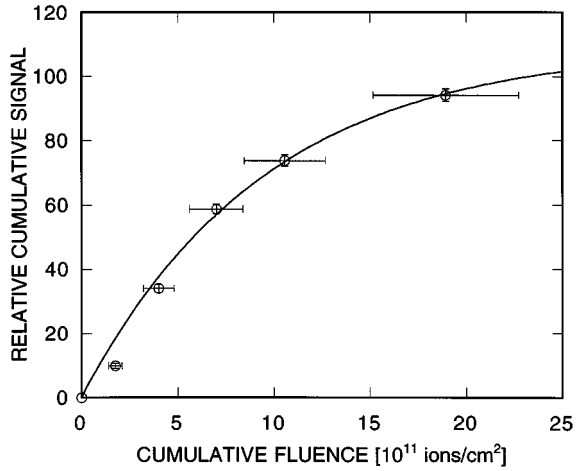

FIG. 3. Characterization of the radiation-induced target damage: One leu_3 target spot was irradiated by 55-MeV ^{127}I ions employing various new collectors. The x axis represents the fluence ϕ on the target and the y axis represents the corresponding cumulative signal obtained by PDMS from the collectors employed up to the fluence ϕ. A least-squares fit of the cumulative signal to Eq. (1) resulted in a damage cross section $\sigma=105\pm21$ nm^2. Error bars of the fluence include errors in beam current and beam spot size. The signal error plotted is the statistical error of mass spectra.

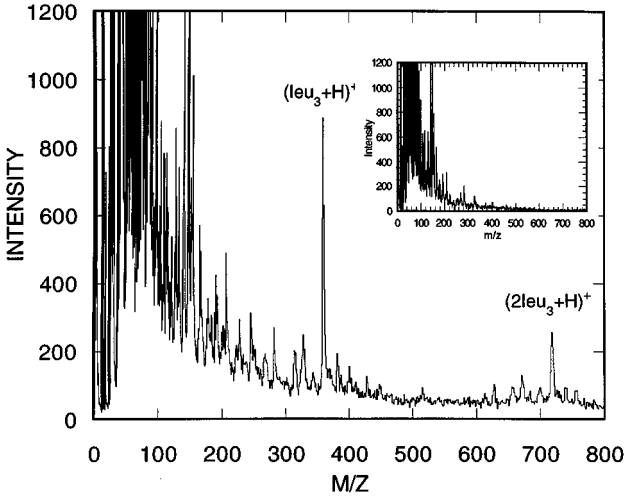

FIG. 4. A typical mass spectrum of a collector employed during target irradiation. The amount of target material on the surface is about 0.4 monolayers as normalized to the amino-acid analysis data. Both the monomer and dimer molecular ion peaks of leu_3 are clearly visible. The inset shows a mass spectrum of the same collector acquired before target irradiation and collection. Ranges of m/z and of intensity per collector incident ion of the two spectra are the same.

were subsequently taken out of the chamber, placed in cleaned test tubes, and subjected to AA.

The flat collector was also employed in a control experiment for the determination of the absolute total sputtering yield. Irradiation ($j\approx35$ pA/mm^2), collection, and subsequent treatment of collector pieces before AA were performed as described above.

It is unknown whether venting the vacuum system before analysis of collectors could alter the distribution of bioorganic material on the collectors. Therefore, an *in situ* angular distribution measurement was also performed, employing the flat collector holder with a 10×50 mm^2 silicon piece during the irradiation ($j\approx55$ pA/mm^2) and with 1.5-mm beam collimators at distances of 0.1 and 0.5 m away from the target. The collector was analyzed by PDMS directly after the target irradiation, without breaking the vacuum. In this case the setup allowed only the y distribution to be monitored.

RESULTS

Target damage

The result of the characterization of the target damaging is shown in Fig. 3. By a least-squares fit to Eq. (1) we obtained $\sigma=105\pm21$ nm^2, close to the value of 144 ± 29 nm^2 obtained for 72-MeV ^{127}I irradiation of leu_3.[31]

Collector response

A typical mass spectrum acquired from a collector is shown in Fig. 4. Both the monomer and the dimer molecular ion peaks are clearly seen. The collector response or PDMS signal as a function of the number of primary ions on the target is shown in Fig. 5(a). In Fig. 5(b) the result of explicitly studying both the monomer and the dimer ion signal from the collector at various depositions on the surface is shown. Detailed comments on these results are given below. Here we note that the response is approximately linear and therefore we can compare the yields in various sputtering angles in a straightforward way. The yield in a sputtering angle interval is simply proportional to the signal from the collector that was located in that angular interval. For the hemispherical collector all angular intervals are of the same size but for the flat holder a compensation for solid angle differences is needed in order to compare the yields in various sputtering angles.

Angular distributions

The y angular distributions as obtained by mass spectrometric analysis of the hemispherical and the flat collectors (compensated for solid angle differences) are shown in Fig. 6. The distributions display symmetry with respect to the target surface normal. Least-squares fits to functions $f_1(\theta)\propto\cos^n(\theta+\theta_0)$, where θ is the polar ejection angle in the yz plane, are characterized by $n=1.32\pm0.20$ and $\theta_0=(2.9\pm2.2)°$ and $n=1.49\pm0.11$ and $\theta_0=(1.0\pm1.0)°$ for the hemispherical and the flat collector, respectively. The material from all five collectors on each side of the normal in the y band was amino-acid analyzed together resulting in one data point for each side. A difference of 25% between the results for the two sides was obtained. Since symmetry was clearly displayed in the PDMS analysis of the y distribution, the error in each point measured by AA was estimated to be approximately $\pm13\%$.

The x angular distribution was clearly asymmetric with respect to the surface normal for both the mass spectrometric and the amino-acid analysis (Fig. 7). The ejection was sharply peaked away from the surface normal and the incident ion direction. A least-squares fit to the function $f_2(\varphi)\propto\cos^m(\varphi+\varphi_0)$, where φ is the polar ejection angle in the xz plane, resulted in $m=4.95$ and $\varphi_0=12.8°$.

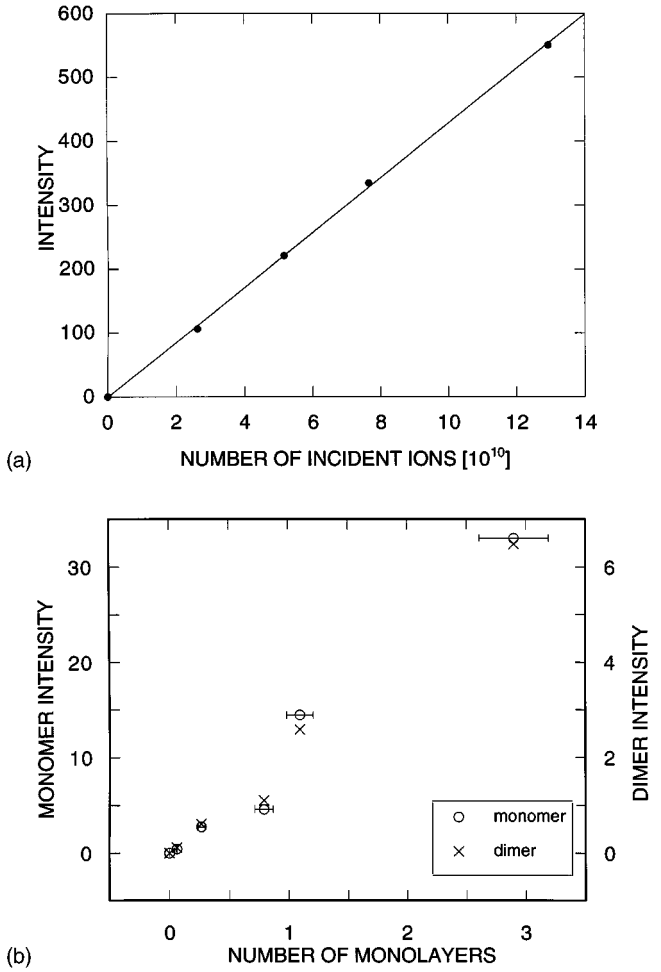

FIG. 5. (a) Collector PDMS signal (response) from one collector as a function of the number of ions incident on various pristine target portions. The solid line represents a linear least-squares fit. (b) Collector response of various collectors exposed to the ejecta while irradiating several pristine target portions. The coverage expressed in monolayers was estimated from the total yield measured by amino-acid analysis and the number of primary ions impinging on the target (see Discussion section). The relative intensity of dimer and monomer signals was constant over a broad range of material deposition on the collector. Error bars of the x axis include errors in beam current and beam spot size but not errors of the amino-acid analysis.

Sputtering yield

In order to estimate the total sputtering yield of leu_3, the angular distributions obtained by PDMS were combined with the AA data. The polar angular coordinates (θ,φ) were converted into ordinary spherical coordinates (θ',φ') by $\theta'=\pi/2-\theta$ (polar angle) and $\varphi'=\pi/2-\varphi$ (azimuthal angle). The amount of sputtered material on the hemispherical collector surface element $d\Omega'=\sin\theta' d\theta' d\varphi'$ is described most generally by a function of the form $F(\theta',\varphi')d\Omega'$. Since the target has an irregular structure,[39] $F(\theta',\varphi')$ is assumed to be separable:

$$F(\theta',\varphi')d\Omega'=Bf_1(\theta')f_2(\varphi')\sin\theta' d\theta' d\varphi'. \quad (2)$$

A least-squares fit of the AA x-band data to Eq. (2) was performed, using $f_1(\theta')$ and $f_2(\varphi')$ from the PDMS angular distribution measurements and B [molecules/rad^2] as the fitting parameter. Hence, the total amount of molecules that would have been collected over the complete hemisphere is

$$C=\int\int_{1/2\ \text{sphere}} Bf_1(\theta')\sin(\theta')d\theta' f_2(\varphi')d\varphi'. \quad (3)$$

C is an estimate since the number of molecules in all solid angle elements of the hemisphere was not measured, and it is a lower bound since the sticking probability of biomolecules on silicon collectors is unknown. In order to estimate the sputtering yield of a pristine target, the damage cross section and the yield as a function of fluence dependence of trileucine was employed to normalize the measured signals. Using I_k from (1) with $\phi_i=0$ and $\phi_{i+1}=\phi_k$ for the kth target spot irradiated, the total number of molecules ejected after irradiating K target spots of area A is

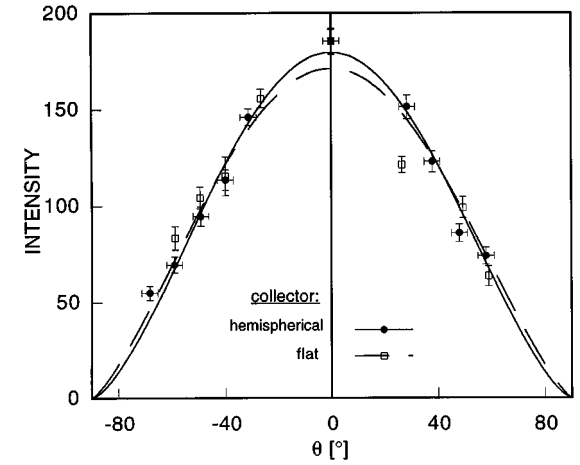

FIG. 6. y angular distributions, $f(\theta)$, of sputtered leu_3 as obtained by mass spectrometric analysis (PDMS) of the hemispherical and flat collectors (compensated for solid angle differences).

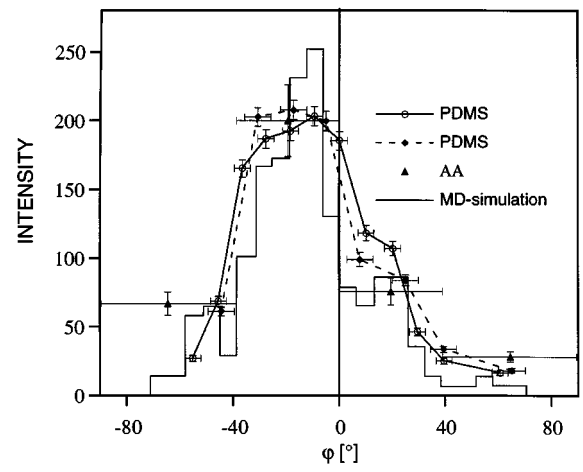

FIG. 7. (a) x angular distributions $f(\varphi)$ of sputtered leu_3 obtained by PDMS and amino-acid collector analyses. The histogram is a result of molecular-dynamics simulation (MD) of a 6-12 Lennard-Jones solid, where a 45° ion incidence target excitation is modeled by expansion of molecules along a 45° angle narrow track (adopted from Ref. 32). The simulation represents a PP-type excitation with molecular collisions in and above the target.

$$C = A \sum_{k=1}^{K} I_k . \quad (4)$$

Since $I_k \propto Y_0$ we could by (4) estimate the sputtering yield of leu_3 to be $Y_0 = (3.5 \pm 1.0) \times 10^3$. For the absolute yield control measurement with the flat collector holder we obtained $Y_0 = (3.1 \pm 1.0) \times 10^3$. Here, a significant part of the sputtered material could not be collected at $\varphi > 0$ and $|\theta| < 0.63$ rad, because of the passage of the ion beam. With aid of the measured angular distributions the loss of material can be estimated and compensated for, which resulted in $Y_0 = (3.6 \pm 1.1) \times 10^3$. The two measurements of Y_0 give an average total yield result: $Y_0 = (3.5 \pm 0.7) \times 10^3$. The agreement between the two measurements is very good. It seems that the collector geometry did not influence the sticking probability. However, not only the geometry but also the current density j was different in the two absolute yield measurements. The independent measurement of the influence by the current density resulted in no differences in the PDMS signals observed from collectors employed as the targets were irradiated at 15, 30, and 60 pA/mm^2. This result confirms the prediction of Ref. 21 that any macroscopic effect caused by the ion beam such as temperature rise or charge up can be neglected at the current densities of the magnitude employed in this experiment. The x distribution is not very well described by $f_2(\varphi)$, which also influences the yield results. The number density of the target $n \approx 2$ nm^{-3}.[31] Using n and Y_0, the volume removed per ion impact is about 2×10^3 nm^3, similar to single ion impact crater volumes measured by SFM for crystalline amino-acid L-valine bombarded by 78-MeV ^{127}I ions.[30] The total yield of leu_3 was larger than previous observations by the collector method for targets composed of the amino-acid leucine, which has a yield of $(1.2 \pm 0.3) \times 10^3$ *assuming* a cosine polar-angle distribution.[22] However, in Ref. 22, no normalization to account for target damage was performed.

The total yield of leu_3 results in negligible gas-phase density of sputtered material. Therefore gas-phase interactions with the incident ion beam that could cause an asymmetry in the angular distribution are excluded at current densities used in these experiments.

DISCUSSION

Experimental challenges

I. Collector response and clusters. The collector response to peptide material deposition or coverage deserves some comments. The average coverage of the collectors in the absolute measurement (AA) with the hemispherical collector ranges from 0.29 to 5.6 monolayers, if we define a monolayer as the number of molecules per unit area with a molecular length $L \approx 0.8$ nm (Ref. 31) and with no overlaps and no empty sites. If we normalize to the AA data we obtain a collector coverage approximately ranging from 0.07 to 1.3 and 0.14 to 2.7 monolayers for the respective xz-plane hemispherical collector data sets analyzed by PDMS. In the spectrum of Fig. 4 it is seen, as in many instances of PDMS of biomolecules, that a dimer ion is present in the spectrum. The surface coverage in this case is ≈ 0.4 monolayers. The ratio between the dimer and monomer ion peak (DMR) was checked for the hemispherical collector data set with the lowest coverage. DMR $= 0.20 \pm 0.05$ over the whole range of sputtering angles measured. In the *in situ* collector response study with collector depositions ranging from 0.06 to 2.9 monolayers we also obtained a coverage independent DMR value [Fig. 5(b)]. This observation is consistent with previous collector experiments on the sputtering of amino-acid leucine.[21] The observed coverage independence of DMR suggests that a large fraction of the objects detected on the collector surface by PDMS are clusters. The clusters could either have been ejected from the target or have resulted from aggregation on the collector surface. The difficulty of detecting individual molecules by PDMS at low surface coverage has been observed at similar vacuum conditions as in the present collector analysis,[44] as well as in UHV environment.[45] Also, the observed *linearity* of the collector response contradicts simple shadowing models[21] for the detection of collected individual molecules on the collector surface. According to such models a saturation of the signal would be observed at the coverage estimated in the response data. If individual molecules were dominating the sputtering yield one would expect an increased slope of the response curve with increased collector coverage, presuming that individual molecules would *not* be detected at low coverage, but *would* be detected when they overlap each other at high coverage. The absence of an increased slope could be explained if individual molecules cannot stick to the collector surface. However, the similarity between the total sputtering yield measured here and the total yield estimates from crater volumes[30] suggests either that there is no preferential sticking of clusters to the collector or that clusters dominate the total yield. The migration and aggregation properties of this adsorption system should be investigated more carefully. However, the present observations of the coverage-independent DMR values, the linear collector response, and the total yield measured suggest that the PDMS signal represents the fraction of molecules contained in sputtered and collected *clusters* and that clusters dominate the total sputtering yield. The amino-acid analysis is *equally sensitive* to amino-acid peptide molecular fragments, whole molecules, and clusters. The similarity in the angular distribution results obtained by AA and PDMS shows that the PDMS signal represents the relative amount of bioorganic material on the collector surface correctly. Collector experiments on 1-MeV/u ^{132}Xe ion bombarded inorganic gypsum targets clearly show ejection of large clusters or ''chunks'' of material.[34] Fission-fragment-induced sputtering of uranium oxide surfaces also exhibit chunk ejection.[33] A detailed and direct imaging of both sputtered biomolecular target and collector surfaces would probably judge whether cluster ejection as suggested by the present results is as prominent also for organic target materials.

II. Erosion of the target. High fluence on the target or irradiation of a large target area is needed in order to obtain reasonably strong signals in PDMS or AA of the collectors. One can estimate that if bombarding an initially smooth surface with fluences similar to those in the present experiment ($> 2 \times 10^{11}$ cm^{-2}), and if the resulting surface track dimensions were similar to that observed on smooth L-valine surfaces ($\approx 10^3$ nm^2),[31] the surface morphology at the end of the irradiation would be very different from the pristine surface. Therefore, angular distribution experiments of the present

type on really smooth surfaces would demand very sophisticated and large scale target scanning if beam-induced surface morphology modification is to be avoided. Electrosprayed surfaces are known to have a somewhat grainy structure.[39] But still, these surfaces are considered as suitable targets for sputter erosion experiments,[21] since the film thickness can be made arbitrarily large and thereby the influence of thickness on the sputtering yield observed for thin films can be avoided.[44] The influence of surface roughness on the angular distribution of ejecta is not understood, but it has been proposed by simulations that a rough surface gives a xz-plane angular distribution with a more ''off-normal'' mean ejection angle than a smooth surface.[13] The fluences per target spot were typically 10×10^{11}, 5×10^{11}, and 2.5×10^{11} [ions/cm^2] for the AA measurement, the first and the second PDMS angular distribution measurements, respectively. However, the observed distributions were similar for the different fluences per target spot employed, which indicates that the surface erosion did not change the angular distribution of sputtered material.

III. Unresolved sputtering angle and kinetic energy. The kinetic energy and the sputtering angle might be correlated. The component of the kinetic energy normal to the adsorbing surface can influence the sticking probability.[46] If the distribution of total kinetic energy were a function of the sputtering angle, ejecta landing on the collector surface with different kinetic energies could result in a distorted angular distribution. For a particular total kinetic energy, a change of the angle at which the ejecta land on the collector surface changes the kinetic energy component normal to the surface. Since the angles at which the ejecta land on the collector at off-normal ejection angles were rather different in the flat and the hemispherical collector experiments, the effect of the normal kinetic-energy component on the sticking probability was in effect probed. Negligible changes of the angular distribution as the angle between the ejecta and the collector surface is changed therefore rule out the possibility that a sputtering-angle-dependent kinetic energy could influence the angular distributions measured.

In spite of the experimental challenges discussed above our results are reproducible, and results obtained with the different approaches are consistent. Also, the angular distribution results presented here are in *qualitative* agreement with a large body of data involving sputtered positive and negative biomolecular *ions*, which also display an off-normal peak ejection angle away from the incident ion direction.[18,47,48]

In most experiments on sputtered biomolecular ions, the actual value of the peak ejection angle is unknown, making quantitative comparison with the present results on the total ejection generally impossible. We note one result on secondary ions of insulin, where the peak ejection angle was estimated at $-50°$,[49] in contrast to our measurement of $-20°$ for leu_3. The source of such a contrast is not now known and raises an important question for future research.

Comparison with models

There are essentially three models making *predictions* about the angular distributions bioorganic material sputtered by fast ions. A *thermal spike* model assumes that the molecules are *evaporated* in a symmetric cosine polar-angular distribution.[10] A ''*phase explosion*'' model assumes that sputtering occurs from a gas jet formed along the track excited by the incident ions.[11] *Pressure pulse* (PP) or *shock wave* (SW) models[50] consider that the ion impact causes a transient energy density gradient which results in impulsive transfer of momentum to the solid, leading to sputtering if the momentum transferred to a molecule is larger than some critical value determined by the binding energy.[12–16] Since the momentum transfer to some location in the target depends on the excitation geometry, the PP/SW models predict a correlation between the ion incidence angle and the angular distribution of sputtered material. The predicted angular distribution is sharply peaked *away* from the direction of the incident ion, i.e., the opposite from the prediction of the ''phase explosion'' model. The observed asymmetric angular distribution in the plane of incidence agrees qualitatively well with predictions by the PP/SW models. The PP/SW model peak ejection angle in the plane of incidence for an incidence angle $\Psi=51°$ is $-19.5°$ $[-(\pi/4-\Psi/2)]$, in good agreement with the observation (Fig. 7). The PP/SW angular prediction considers only ejection from the surface. Broadening of angular distributions can occur as a result of collisions between the ejecta in the vicinity of the surface. Molecular-dynamics simulations by Fenyö *et al.*[13,32] of a 6-12 Lennard-Jones solid excited by a narrow track expansion provide information on angular distributions in a case of PP-type excitation with some degree of intermolecular collisions above the surface. Molecules of mass 10^4 u and a 45° expanding track result in an angular distribution of sputtered molecules in the plane of incidence[32] very similar to the present experimental result (Fig. 7).

In the very simplest form of the PP model the critical momentum, which is a necessary condition for sputtering, is obtained at a critical radius r_c inside which ejection can take place, and r_c is independent of the mass of the objects removed.[12,13] Recently, in a more detailed treatment of the PP model, it was shown that larger sputtered objects, i.e., clusters, can be favored in PP sputtering, especially for off-normal ion angle of incidence.[51] In the thermal spike model the flux of particles evaporating from the surface is $\propto M^{-3/2}\exp(-\alpha M^{2/3}\varepsilon^{-1})$, where α is a constant, ε is the energy density, and M is the mass of the evaporating objects.[17] It is seen from this relation that thermal spike ejection of large species such as clusters is clearly unfavorable. Therefore, preferential cluster ejection, as indicated by the present experiments, is reasonably explained if fast-ion-induced sputtering of intact biomolecules is mainly due to a hydrodynamic type of mechanism rather than to an evaporative thermal spike process.

CONCLUSIONS

The total sputtering of a peptide surface induced by incident fast atomic ions was studied. A peptide tri-leucine surface bombarded by 55-MeV ^{127}I ions resulted in angular distributions of sputtered peptide material sharply peaked away from the surface normal and the ion incidence direction in the plane of incidence, while the distribution in the plane perpendicular to the incidence plane was normally peaked and symmetric. The angular distributions measured show that the large body of data existing for biomolecular *ions*

qualitatively correctly reflect the overall fast-ion-induced biomolecular ejection. Total sputtering yields of the order of 10^3 peptide molecules per incident ion were detected, similar to observations on other bioorganic targets, and a large fraction of the total sputtering yield appeared to come from ejected clusters. The observations agree with predictions of the pressure pulse or shock wave models, which assume an impulsively driven ejection mechanism for describing the fast-ion-induced sputtering of organic solids.

ACKNOWLEDGMENTS

C. T. Reimann is acknowledged for fruitful discussions and valuable criticism of the manuscript. J. Kjellberg and J. Åström are thanked for technical assistance. U. Jansson and M. Sundqvist provided the surface cleaning and the amino-acid analysis facilities, respectively. This work was supported by the Swedish Natural Sciences Research Council (NFR) and the Ångström consortium.

[1] B. Sundqvist and R. D. Macfarlane, Mass Spectom. Rev. **4**, 421 (1985).
[2] P. Håkansson, Det Kgl. Danske Videnskab. Selskab Mat. Fys. Medd. **43**, 593 (1993).
[3] M. P. Waligórski, R. N. Hamn, and R. Katz, Nucl. Tracks Radiat. Meas. **11**, 309 (1986).
[4] R. M. Papaléo, P. Demirev, J. Eriksson, P. Håkansson, B. U. R. Sundqvist, and R. E. Johnson, Phys. Rev. Lett. **77**, 667 (1996).
[5] T. A. Tombrello, Nucl. Instrum. Methods Phys. Res. B **2**, 555 (1984).
[6] A. Hedin, P. Håkansson, B. U. R. Sundqvist, and R. Johnson, Phys. Rev. B **31**, 1780 (1985).
[7] R. L. Fleischer, P. Price, and R. M. Walker, *Nuclear Tracks in Solids* (Univ. of California Press, Berkeley, 1975).
[8] D. Albrecht, P. Armbruster, R. Spohr, M. Roth, K. Schaupert, and H. Stuhrmann, Appl. Phys. A **37**, 37 (1985).
[9] T. A. Tombrello, Nucl. Instrum. Methods Phys. Res. B **94**, 424 (1994).
[10] I. NooreBateha, R. R. Lucchese, and Y. Zuri, J. Chem. Phys. **86**, 5816 (1988).
[11] R. R. Lucchese, J. Chem. Phys. **86**, 443 (1987).
[12] R. E. Johnson, B. U. R. Sundqvist, A. Hedin, and D. Fenyö, Phys. Rev. B **40**, 49 (1989).
[13] D. Fenyö and R. E. Johnson, Phys. Rev. B **46**, 5090 (1992).
[14] I. S. Bitensky, A. M. Goldenberg, and E. S. Parilis, J. Phys. (Paris) Colloq. **50**, C2-213 (1989).
[15] I. S. Bitensky, A. M. Goldenberg, and E. S. Parilis, in *Ion Formation from Organic Solids V*, edited by A. Hedin, B. U. R. Sundqvist, and A. Benninghoven (Wiley, New York, 1990), p. 205.
[16] I. S. Bitensky, A. M. Goldberg, and E. S. Parilis, in *Methods and Mechanisms for Producing Ions from Large Molecules*, edited by K. G. Standing and W. Ens (Plenum, New York, 1991), p. 83.
[17] C. T. Reimann, Det Kgl. Danske Videnskab. Selskab Mat. Fys. Medd. **43**, 351 (1993).
[18] R. Moshammer, R. Matthäus, K. Wien, and G. Bolbach, in *Ion Formation from Organic Solids V* (Ref. 15), p. 17.
[19] D. Fenyö, A. Hedin, P. Håkansson, and B. U. R. Sundqvist, Int. J. Mass Spectrom. Ion Proc. **100**, 63 (1990).
[20] W. Ens, B. U. R. Sundqvist, P. Håkansson, D. Fenyö, A. Hedin, and G. Jonsson, J. Phys. (Paris) Colloq. **50**, C2-9, (1989).
[21] A. Hedin, P. Håkansson, M. Salehpour, and B. U. R. Sundqvist, B **35**, 7377 (1987).
[22] M. Salehpour, P. Håkansson, B. Sundqvist, and S. Widdiyasekera, Nucl. Instrum. Methods Phys. Res. B **13**, 278 (1986).
[23] S. Bouffard, J. Cousty, Y. Pennec, and F. Thibaudau, Rad. Eff. Defects Solids **126**, 225 (1993).
[24] C. Tomaschko, M. Schurr, R. Berger, G. Saemann-Ischenko, H. Voit, A. Brunelle, S. Della-Negra, and Y. LeBeyec, Rap. Commun. Mass Spectrom. **9**, 924 (1995).
[25] D. D. N. B. Daya, A. Hallén, P. Håkansson, B. U. R. Sundqvist, and C. T. Reimann, Nucl. Instrum. Methods Phys. Res. B **103**, 454 (1995).
[26] D. D. N. B. Daya, A. Hallén, J. Eriksson, J. Kopniczky, R. Papaléo, C. T. Reimann, P. Håkansson, B. U. R. Sundqvist, A. Brunelle, S. Della-Negra, and Y. L. Beyec, Nucl. Instrum. Methods Phys. Res. B **106**, 38 (1995).
[27] J. Kopniczky, C. T. Reimann, A. Hallén, B. U. R. Sundqvist, P. Tengvall, and R. Erlandsson, Phys. Rev. B **49**, 625 (1994).
[28] J. Kopniczky, A. Hallén, N. Keskitalo, C. T. Reimann, and B. U. R. Sundqvist, Rad. Meas. **25**, 47 (1995).
[29] C. T. Reimann, J. Kopniczky, E. Wistus, J. Eriksson, P. Håkansson, and B. U. R. Sundqvist, Int. J. Mass Spectrom. Ion Proc. **151**, 147 (1995).
[30] J. Eriksson, J. Kopniczky, G. Brinkmalm, R. M. Papaléo, P. Demirev, C. T. Reimann, P. Håkansson, and B. U. R. Sundqvist, Nucl. Instr. Meth. Phys. Res. B **101**, 142 (1995).
[31] J. Eriksson, J. Kopniczky, P. Demirev, R. M. Papaléo, G. Brinkmalm, C. T. Reimann, P. Håkansson, and B. U. R. Sundqvist, Nucl. Instrum. Methods Phys. Res. B **107**, 281 (1996).
[32] D. Fenyö, B. U. R. Sundqvist, B. Karlsson, and R. E. Johnson, Phys. Rev. B **42**, 1895 (1990).
[33] J. P. Biersack, D. Fink, and P. Mertens, J. Nucl. Mater. **53**, 194 (1974).
[34] I. V. Vorobyova, V. E. Monastyrenko, and V. P. Perelygin, Sov. Phys. Solid State **28**, 1343 (1984).
[35] I. V. Vorobyova and E. A. Ter-Ovanes'yan, Sov. Phys. Solid State **34**, 222 (1992).
[36] J. E. Griffith, R. E. Weller, L. E. Seiberling, and T. A. Tombrello, Radiat. Eff. **51**, 223 (1980).
[37] D. H. Spackman, W. H. Stein, and S. Moore, Anal. Chem. **30**, 1190 (1958).
[38] E. Bruninx and G. Rudstam, Nucl. Instrum. Methods Phys. Res. **13**, 131 (1961).
[39] G. Säve, P. Håkansson, and B. U. R. Sundqvist, Anal. Chem. **59**, 2059 (1987).
[40] W. Kern, J. Electrochem. Soc. **137**, 1887 (1990).
[41] M. Salehpour, P. Håkansson, and B. Sundqvist, Nucl. Instrum. Methods Phys. Res. B **2**, 752 (1984).
[42] R. M. Papaléo, A. Hallén, J. Eriksson, G. Brinkmalm, P. Demirev, P. Håkansson, and B. U. R. Sundqvist, Nucl. Instrum. Methods Phys. Res. B **91**, 124 (1994).
[43] H. D. Betz, Rev. Mod. Phys. **44**, 465 (1972).
[44] G. Säve, P. Håkansson, and B. U. R. Sundqvist, Nucl. Instrum. Methods Phys. Res. B **26**, 571 (1987).

[45] M. Wagner, K. Wien, B. Curdes, and E. R. Hilf, Nucl. Instrum. Methods Phys. Res. B **82**, 362 (1993).

[46] A. Zangwill, *Physics at Surfaces* (Cambridge University Press, Cambridge, 1988).

[47] W. Ens, B. U. R. Sundqvist, P. Håkansson, A. Hedin, and G. Jonsson, Phys. Rev. B **39**, 763 (1989).

[48] D. Fenyö, A. Hedin, P. Håkansson, R. E. Johnson, and B. U. R. Sundqvist, in *Ion Formation from Organic Solids V* (Ref. 15), p. 33.

[49] D. Fenyö, B. U. R. Sundqvist, B. Karlsson, and R. E. Johnson, J. Phys. (Paris) Colloq. **50**, C2-33 (1989).

[50] PP and SW models both assume that a transient energy density gradient results in impulsive transfer of momentum to the molecules. The SW model assumes the formation of a shock wave around and along the ion track and an acoustic-type wave propagation for the energy transport to the solid, whereas the PP model assumes the formation of closely spaced spherical sources of energy along the track from which the energy propagates according to a diffusion equation (see Refs. 12–17).

[51] C. T. Reimann, Nucl. Instrum. Methods Phys. Res. B **95**, 181 (1995).